THE INFLUENCE OF SPATIAL VARIABILITY ON THE GEOTECHNICAL DESIGN PROPERTIES OF A STIFF, OVERCONSOLIDATED CLAY

Mark B. Jaksa

B.E.(Hons), M.I.E.(Aust), CPEng

THESIS SUBMITTED FOR THE DEGREE OF
DOCTOR OF PHILOSOPHY

in

The University of Adelaide
(Faculty of Engineering)

December 1995

To my wife Marie,

and my parents Stan and Maria

Preface

The work described in this thesis was undertaken over the period of 7½ years, between February 1988 and October 1995, within the Department of Civil and Environmental Engineering, at the University of Adelaide. Throughout the thesis, all materials, techniques, concepts and conclusions obtained from other sources have been acknowledged in the text. Listed below are those sections of the thesis for which, to the best of his knowledge, the author claims originality, as well as papers which have been published as a direct result of this study.

In **Chapter 3**:

- the design and development of the hardware of the micro-computer based data acquisition system used for the cone penetration tests. The hardware was designed in collaboration with Mr. Bruce Lucas of the Department of Civil and Environmental Engineering, The University of Adelaide;

- the complete design and development of the computer programs: *CPTest*; *CPTView*; *CPTPlot*; and *CPTPrint*, associated with the CPT data acquisition system;

- the data transformation technique of *depth rationalisation*.

In **Chapter 4**:

- the measurement of closely-spaced CPT data, both vertically and laterally, to enable the small-scale spatial variability of undrained shear strength to be examined;

- the design, development and implementation of the horizontal cone penetration test performed at the Keswick site. The design and testing was performed in collaboration with undergraduate students Dirk van Holst Pellekaan and Julian Cathro.

In **Chapter 5**:

- the complete design and development of the computer programs: *SemiAuto*; *CPTSpace*; and *Monte*;
- the association between the correlation distance, the scale of fluctuation, δ_v, and Bartlett's limits, r_B, as well as the development of relationships between a, r_B and δ_v;
- recognition of the *rebound phenomenon* associated with sleeve friction measurements in the Keswick Clay, as well as the use of the cross-correlation function to quantify the *shift distance* associated with the CPT;
- development of a nested semivariogram model to represent the lateral spatial variation of the undrained shear strength of the Keswick Clay;
- identification of factors which result in inaccuracies with respect to Baecher's technique for the evaluation of random measurement errors;
- the use of rescaled residuals in the random field theory estimation process;
- the use of random field theory to forecast and simulate geotechnical data;
- the use of geostatistics to estimate and forecast geotechnical data.

In **Chapter 6**:

- the complete development of *KESWICK*, the data base of geotechnical properties of the Keswick and Hindmarsh Clays.

In **Chapter 7**:

- the development of the framework to provide preliminary estimates of the undrained shear strength of the Keswick Clay.

In **Chapter 8**:

- the complete design and development of the computer program: *LCPCSim*;

- the significance of the spatial variability of undrained shear strength in the design of piled foundations;

- the use of geostatistical simulation techniques to generate data to enable the influence of spatial variability of undrained shear strength on the design of piled foundations to be examined.

A list of publications that have been prepared as a result of this research is presented below.

Jaksa, M. B. and Kaggwa, W. S. (1992). Degree of Saturation of the Keswick Clay Within the Adelaide City Area Above the General Groundwater Table. *Proc. 6th Australia New Zealand Conf. on Geomechanics*, Christchurch, pp. 336-341.

Kaggwa, W. S. and Jaksa, M. B. (1992). Normalised Shear Strength and Compressibility Characteristics of Adelaide Expansive Clay. *Proc. 6th Australia New Zealand Conf. on Geomechanics*, Christchurch, pp. 330-335.

Jaksa, M. B., Kaggwa, W. S. and Brooker, P. I. (1993). Geostatistical Modelling of the Undrained Shear Strength of a Stiff, Overconsolidated, Clay. *Proceedings of Conference of Probabilistic Methods in Geotechnical Engineering*, Canberra, pp. 185-194.

Jaksa, M. B. (1994). *CPTSuite User Manual*. Dept. Civil & Env. Engrg., Uni. of Adelaide, 30 p.

Jaksa, M. B., Brooker, P. I. and Kaggwa, W. S. (1994). Inaccuracies Associated with the Current Method for Estimating Random Measurement Errors. *Research Report No. R 122*, Dept. Civil & Env. Engrg., Uni. of Adelaide, December, 28 p.

Jaksa, M. B., Brooker, P. I., Kaggwa, W. S., van Holst Pellekaan, P. D. A. and Cathro, J. L. (1994). Modelling the Lateral Spatial Variation of the Undrained Shear Strength of a Stiff, Overconsolidated Clay Using an Horizontal Cone Penetration Test. *Research Report No. R 117*, Dept. Civil & Env. Engrg., Uni. of Adelaide, September, 34 p.

Jaksa, M. B. and Kaggwa, W. S. (1994). A Micro-Computer Based Data Acquisition System for the Cone Penetration Test. *Research Report No. R 116*, Dept. Civil & Env. Engrg., Uni. of Adelaide, 31 p.

Jaksa, M. B. and Kaggwa, W. S. (1994). Geotechnical Engineering Software Recently Developed at the University of Adelaide. *Australian Geomechanics*, No. 26, October, pp. 33-38.

Jaksa, M. B. and Lucas, B. (1995). *CPT-DAS: Cone Penetration Test Data Acquisition System User Manual*. CIVILTEST, Dept. Civil & Env. Engrg., Uni. of Adelaide, 12 p.

Abstract

The research presented in this thesis focuses on the spatial variability of the Keswick and Hindmarsh Clays within the Adelaide city area. Keswick Clay is locally significant since many of Adelaide's multi-storey buildings are founded directly on it, and internationally significant, since it has been shown by Cox (1970), that this clay exhibits remarkably similar properties to those of the well-documented London Clay.

The assessment of the small-scale variability of the undrained shear strength of these clays is based on measurements obtained using the electrical cone penetration test (CPT), and a micro-computer based data acquisition system, designed specifically for this study. A significant feature of the data acquisition system is that it enables measurements to be obtained at intervals of 5 mm, both reliably and efficiently. The development of the data acquisition system is discussed, and the accuracy of its measurements is examined. The small-scale variability of the undrained shear strength of the Keswick Clay is based on more than 200 vertical CPTs, performed within an area of 50×50 metres at a site located in the Adelaide city area. The CPTs were spaced at lateral intervals varying between 0.5 and 5 metres, with each vertical CPT extending to a typical depth of 5 metres. In addition, the small-scale horizontal spatial variability of the Keswick Clay is examined using an electrical cone penetrometer driven horizontally into the face of an embankment, again located within the Adelaide city area. The accuracy of the CPT measurements is examined, and discussion is given of the shortcomings associated with a commonly used technique, by Baecher (1982), for estimating the random measurement error associated with various test procedures.

The assessment of the large-scale spatial variability of the undrained shear strength of the Keswick and Hindmarsh Clays is founded on a data base of geotechnical engineering properties, compiled from a number of consulting engineering practices and government instrumentalities. The data base, known as *KESWICK*, contains approximately 160 site investigations, 380 boreholes, and 10,140 measurements obtained from a number of different laboratory and in situ tests. In addition, *KESWICK* is used to establish generalised

trends and bounds, associated with the various geotechnical engineering design properties contained within the data base.

The techniques of random field theory and geostatistics are used to quantify, model and predict the spatial variability of the Keswick and Hindmarsh Clays. These techniques are compared with one another in order to assess the suitability and shortcomings of each, when applied to the study of the spatial variability of geotechnical engineering materials. Furthermore, a number of specifically-written computer programs, which were developed to enable the various spatial variability analyses to be performed, are discussed. It is demonstrated that the lateral undrained shear strength of the Keswick Clay, within the Adelaide city area, exhibits a nested structure; that is, one which is the compound effect of several genetic sources of spatial variation. In addition, it is shown that this nested structure can be adequately modelled by means of a spherical semivariogram model.

The nested structure is used, together with the kriging estimation process, to provide preliminary estimates of the undrained shear strength of the Keswick Clay, within the Adelaide city area. The analyses demonstrate that the nested model and the kriging process provide a useful facility for generating preliminary estimates of the strength of the clay.

Finally, the significance of the spatial variability of the undrained shear strength of clay soils is examined, with reference to the design of embankments and pile foundations. It is demonstrated that the correlation distance can greatly influence the design of each of these geotechnical systems.

Statement of Originality

This thesis contains no material which has been accepted for the award of any other degree or diploma in any university or other tertiary institution and, to the best of my knowledge and belief, contains no material previously published or written by another person, except where due reference has been made in the text.

I give consent to this copy of my thesis, when deposited in the University Library, being made available for loan and photocopying.

Signed: Date: 19/12/95.....

Acknowledgments

This PhD research began in February 1988 and has been carried out on a part-time basis ever since. I owe an enormous debt of gratitude to my supervisors, Dr. William Kaggwa, of the Department of Civil and Environmental Engineering, and Dr. Peter Brooker, of the Department of Geology and Geophysics, for their time, patience, guidance and continual support throughout this research programme. In addition, their advice and encouragement have been of great value to me, and this thesis would not have been possible but for their contribution. The assistance of Prof. Stephen Priest and Dr. J. Neil Kay in the first two years of this project is also greatly appreciated. In addition, I wish to thank Dr. Ari Verbyla and the late Dr. W. B. Taylor, of the Department of Statistics, for their patience and assistance with respect to time series analysis and related techniques.

I wish to thank the Department of Civil and Environmental Engineering for their continual support and patience during my candidature. I wish to acknowledge the enormous support given to me by Mr. Tad Sawosko who spent many weeks, and long, tiring days, in the field performing the 223 cone penetration tests. In addition, Tad's suggestions, laboratory support and warm nature, are gratefully acknowledged. The micro-computer based data acquisition system was developed, largely as the result of the electronic expertise of Mr. Bruce Lucas. His support and dedication to this research programme is greatly appreciated. In addition, I wish to thank other members of the Department's technical staff, in particular: Messrs. Stan Woithe; Werner Eidam; Colin Haese; Robert Kelman; Laurie Collins; and Ms Deborah Hammond, who each contributed to this research in one form or another.

The field study was carried out with the generous support of the Department of Transport and the Adelaide City Council. I thank both of these organisations, and in particular, Messrs. Roman Washyn, Richard Herraman, Ian Forrester and Mark Underhill for their significant contribution to this study. In addition, I am grateful for the generosity and assistance provided by Australian National, and in particular, Mr. Peter Gaskill, for allowing testing to be carried out at the Keswick site. I also wish to thank Dr. K. S. Li, Mitchell, McFarlane, Brentnall and Partners, Hong Kong, and Dr. S.-C. R. Lo and Mr. G. R. Mostyn, University of N.S.W., for permission to use the program *PROBSN*.

I wish to acknowledge the assistance and kindness of the following organisations and individuals for allowing their test information and job files to be inspected so that the *KESWICK* data base could be compiled:

Coffey Partners International Pty. Ltd.	I. Hosking. R. Grounds
Connell Wagner (SA) Pty. Ltd.	G. Benny, W. Graham
Golder Associates Pty. Ltd. *(formerly Woodburn Fitzhardinge Geotechnical)*	C. Fitzhardinge, I. Shipway
ACER Wargon Chapman (SA) Pty. Ltd. *(formerly Hosking Oborn Freeman and Fox)*	R. Stevens
Kinhill Engineers	R. Perry
Koukourou and Partners	P. Bayetto, R. Bryant, P. Lambert, Q. Jones
Rust PPK Consultants Pty. Ltd. *(formerly PPK Consultants Pty. Ltd.)*	P. Mitchell
SACON	S. Wawryk, L. Sanders

Considerable assistance was given to me via the Cathie Fund, in the form of a series of Release Time Scholarships, which allowed me to be released from some of my teaching duties, and hence enabled me to devote more time to my PhD research. I wish to thank all who assisted me in this regard, particularly Ms Sharon Mosler. In addition, I wish to acknowledge the assistance of the S.A. Department of Environment and Natural Resources, and in particular, my brother Daniel for the map of Australia, as well as invaluable surveying advice; Mr. Malcolm Sheard from the Mines and Energy, S.A. for useful information regarding the Keswick and Hindmarsh Clays; and Mr. Mike Vowles of the Bureau of Meteorology for the climatic data presented in Chapter 4.

I wish to thank fellow postgraduate students: Philip Crawley; Tony Meyers; and Holger Maier for their friendship, encouragement and advice. In addition, thanks are also due to Paul Morgan, and my wife, Marie, for proof-reading the thesis.

Since 1992, a series of enthusiastic and capable final year, undergraduate students assisted with various aspects of this research. I wish to thank Stuart Potter, Phuc Do, Dirk van Holst Pellekaan, Julian Cathro, Rachel Hawtin, Lynn Lim, Greg Dufour, and Kelly Manning for their contributions to this research.

Finally, I will always be indebted to my family, particularly my wife, Marie, for her constant love, sacrifice and support throughout the period of my candidature, and my parents, Stan and Maria, for the considerable sacrifices which they have made on my behalf throughout my life. Lastly, I am indebted to my Lord for the strength, nourishment and opportunities which I have been blessed with during this period of study.

Contents

Note: All blank pages have been given page numbers.

Preface ..... *i*
Abstract ..... *iv*
Statement of Originality ..... *vi*
Acknowledgments ..... *vii*
Contents ..... *ix*
List of Figures ..... *xv*
List of Tables ..... *xxvi*
Notation ..... *xxx*
Glossary ..... *xxxviii*

Chapter 1. Introduction 1
1.1 INTRODUCTION 1
1.2 AIMS AND SCOPE OF THESIS 3
1.3 LAYOUT OF THESIS 6

Chapter 2. Literature Review 8
2.1 INTRODUCTION 8
2.2 THE STUDY AREA 8
2.3 KESWICK AND HINDMARSH CLAYS 9
2.3.1 Geological History 9
2.3.2 Geotechnical Characteristics 13
2.3.2.1 Stratigraphy 14
(i) Keswick Clay 14
(ii) Hindmarsh Clay Sand Member 15
(iii) Hindmarsh Clay Layer 16
2.3.2.2 Mineralogy 16
2.3.2.3 Plasticity 18
2.3.2.4 Moisture Regime 18
2.3.2.5 Specific Gravity 19
2.3.2.6 Degree of Saturation 19
2.3.2.7 Instability Index, I_{pt} 20
2.3.2.8 Coefficient of Earth Pressure at Rest, K_0 20
2.3.3 Structural Features 21
2.3.3.1 Gilgais 22

2.3.4 Groundwater....24
2.3.5 Summary....25
2.4 THE CONE PENETRATION TEST....25
2.4.1 Introduction....25
2.4.2 Equipment....26
2.4.3 Procedure....28
2.4.4 Applications and Data Interpretation....29
2.4.5 Determination of the Undrained Shear Strength of a Clay from the CPT....30
2.4.6 Extent of the Failure Zone Due to Cone Penetration....34
2.4.7 Accuracy of the CPT....35
2.4.7.1 Equipment Errors of the CPT....36
2.4.7.2 Operator/Procedural Errors of the CPT....37
2.4.7.3 Random Errors of the CPT....38
2.4.7.4 Total Measurement Errors of the CPT....39
2.4.8 Summary....39
2.5 SPATIAL VARIABILITY OF SOILS....39
2.5.1 Mathematical Techniques Used to Model Spatial Variability....40
2.5.1.1 Regression Analysis....40
2.5.1.2 Random Field Theory....44
(i) Stationarity....44
(ii) Data Transformation....46
(iii) Autocovariance and the Autocorrelation Function....48
(iv) Partial Autocorrelation Function....51
(v) Estimation - Random Field Models....52
(vi) Cross-Covariance and the Cross-Correlation Function....59
2.5.1.3 Geostatistics....60
(i) Semivariogram....61
(ii) Estimation - Kriging....65
2.5.1.4 Tests for Non-Stationarity....69
2.5.2 Historical Studies Concerned with the Spatial Variability of Geotechnical Materials....73
2.5.2.1 Random Field Theory....74
2.5.2.2 Geostatistical Analyses....96
2.6 SUMMARY....100

Chapter 3. Development of a Micro-Computer Based Data Acquisition System for the Cone Penetration Test....101
3.1 INTRODUCTION....101
3.2 EXISTING DATA ACQUISITION SYSTEMS....101

3.3 DESIGN CRITERIA FOR DATA ACQUISITION SYSTEM 104
3.4 DESIGN AND CONSTRUCTION OF UNIVERSITY OF ADELAIDE DATA ACQUISITION SYSTEM 105
3.4.1 Equipment 105
3.4.1.1 Electric Cone Penetrometer 105
3.4.1.2 Depth Box 105
3.4.2 Measurement and Recording 107
3.4.2.1 Hardware 107
(i) Microprocessor Interface 107
(ii) Micro-Computer 109
(iii) Alarm Button 109
3.4.2.2 Software 110
(i) *CPTRead* 111
(ii) *CPTest* 112
3.4.3 Post-Processing 115
3.4.3.1 *CPTView* 115
3.4.3.2 *CPTPlot* 115
3.4.3.3 *CPTPrint* 121
3.4.4 Description of Overall Data Acquisition System 121
3.5 CALIBRATION AND ACCURACY OF EQUIPMENT 123
3.5.1 Resolution of Measured Data 123
3.5.2 Calibration Tests to Quantify Measurement Errors 123
3.5.2.1 Depth Box and Depth Measurements 124
3.5.2.2 Measurements of q_c and f_s 125
3.5.2.3 Microprocessor Interface Sampling Rate 126
3.5.3 Random Measurement Errors 126
3.6 FIELD PERFORMANCE 127
3.6.1 Falling Off 127
3.6.2 Noise Spikes 129
3.6.3 Limitations of Data Acquisition System 129
3.7 SUMMARY 129

Chapter 4. Experimental Programme 131
4.1 INTRODUCTION 131
4.2 LOCATION OF SITE FOR FIELD STUDY 131
4.3 FIELD TESTING - SOUTH PARKLANDS SITE 132
4.3.1 Layout of Field Testing 132
4.3.2 Equipment and Methods 135
4.3.3 Sampling and Logging 139
4.3.4 Reduction of Errors During Field Testing 141

4.3.5 Level Survey of South Parklands Site 143
4.4 FIELD TESTING - KESWICK SITE 148
4.4.1 Location of Site for Horizontal Spatial Variability Field Study 149
4.4.2 Horizontal CPT Equipment and Methods 150
4.5 DETERMINATION OF CONE FACTOR, N_k 155
4.6 SUMMARY 166

Chapter 5. Examination of the Small-Scale Spatial Variability of the Keswick Clay 167
5.1 INTRODUCTION 167
5.2 DEVELOPMENT OF SOFTWARE 167
5.2.1 *SemiAuto* 167
5.2.2 *Monte* 169
5.2.3 *CPTSpace* 171
5.3 ANALYSIS OF SPATIAL VARIABILITY OF KESWICK CLAY 171
5.3.1 Vertical Spatial Variability 172
5.3.1.1 Random Field Theory Analyses 176
5.3.1.2 Geostatistical Analyses 183
5.3.1.3 Spatial Variability Models Derived From s_u Compared With q_c 189
5.3.2 Horizontal Spatial Variability 192
5.3.2.1 South Parklands Site 192
5.3.2.2 Keswick Site 202
5.3.2.3 Discussion of Horizontal Spatial Variability Results 205
5.3.3 Relationship Between δ_v, r_B and a 211
5.3.4 Analysis of Sleeve Friction Measurements 213
5.3.5 Cross-Correlation Analysis: q_c and f_s 220
5.3.6 Discussion of Spatial Variability Results 225
5.3.7 Summary 228
5.4 MODEL FORMULATION, PARAMETER ESTIMATION, FORECASTING AND DATA SIMULATION 229
5.4.1 Random Field Theory 230
5.4.1.1 Re-examination of Ravi's (1992) Analysis 230
5.4.2 Random Field Analyses of Keswick Clay 234
5.4.2.1 Model Formulation and Parameter Estimation 234
5.4.2.2 Forecasting 247
5.4.2.3 Data Simulation 249
5.4.3 Geostatistical Analyses 254
5.4.3.1 Forecasting 254

5.4.4 Summary of Random Field and Geostatistical Modelling of Keswick Clay 265
5.5 ASSESSMENT OF ACCURACY OF MEASURED DATA....266
5.5.1 Inadequacies of Baecher's Method 266
5.5.1.1 Nugget Effect 267
5.5.1.2 Sample Spacing....267
5.5.1.3 Trend Removal from Data....268
5.5.2 Case Studies....268
5.5.2.1 Sensitivity of Vertical Spatial Variability 269
(i) Effect of Trend Removal....269
(ii) Effect of Sample Spacing 270
5.5.2.2 Sensitivity of Horizontal Spatial Variability 274
(i) Effect of Trend Removal....274
(ii) Effect of Sample Spacing 274
5.5.3 Conclusions....278
5.6 SUMMARY 279

Chapter 6. Compilation of a Data Base of Geotechnical Properties of the Keswick and Hindmarsh Clays 282
6.1 INTRODUCTION 282
6.2 GEOTECHNICAL DATA BASES DISCUSSED IN THE LITERATURE....282
6.3 FORMULATION OF THE *KESWICK* DATA BASE....284
6.4 DESCRIPTION OF THE *KESWICK* DATA BASE....285
6.5 APPLICATION OF THE *KESWICK* DATA BASE....291
6.5.1 Contours of Layer Surfaces 291
6.5.2 Moisture and Density Relationships with Depth....292
6.5.3 Specific Gravity and Degree of Saturation 301
6.5.4 Shear Strength....305
6.5.5 Young's Modulus of Elasticity 312
6.5.6 SPT Number 315
6.5.7 Soil Suction....317
6.5.8 Contours of Undrained Shear Strength 318
6.6 SUMMARY 324

Chapter 7. Examination of the Large-Scale Lateral Spatial Variability of the Keswick Clay 325
7.1 INTRODUCTION 325
7.2 INPUT DATA AND TRANSFORMATIONS 325
7.3 GEOSTATISTICAL MODEL....329

7.4 ASSESSMENT OF THE GEOSTATISTICAL MODEL 336
7.4.1 Cross Validation Analyses 336
7.4.2 Ordinary Kriging Analyses 339
7.5 SUMMARY 348

Chapter 8. Significance of Spatial Variability with Respect to Geotechnical Engineering Design 349
8.1 INTRODUCTION 349
8.2 SLOPE STABILITY ANALYSIS 349
8.3 PILE DESIGN 352
8.3.1 LCPC Method 353
8.3.2 Hypothetical Field Problems 355
8.3.2.1 South Parklands Site 355
8.3.2.2 Simulated Data 360
8.4 SUMMARY 370

Chapter 9. Summary and Conclusions 372
9.1 SUMMARY 372
9.2 RECOMMENDATIONS FOR FURTHER RESEARCH 376
9.3 CONCLUSION 378

References 379

Appendix A Selected Cone Penetration Test Results from Field Study 397

Appendix B Engineering Borehole Logs 443

Appendix C Data Base of the Geotechnical Properties of the Keswick and Hindmarsh Clays 451

List of Figures

Chapter 2. Literature Review

2.1 Locality plan 9
2.2 The Adelaide city area 10
2.3 The St. Vincent basin 12
2.4 Distribution of the Keswick Clay 15
2.5 Distribution of the Hindmarsh Clay 17
2.6 Typical gilgai structures within the Adelaide city area 23
2.7 Suggested origin of gilgai structures 24
2.8 Schematic diagram of the electric cone penetrometer 27
2.9 Schematic representation of r_p and z_p 34
2.10 Location of the elasto-plastic boundary in cone penetration 35
2.11 Hypothetical sedimentary rock data showing straight lines fitted by different methods 42
2.12 An example of a non-stationary data set 45
2.13 Forms of non-stationarity: (a) trend non-stationarity, (b) variance non-stationarity, (c) relationship non-stationarity 46
2.14 Summary of the Box-Jenkins procedure 53
2.15 Relationship between the semivariogram, γ_h, and the autocorrelation, ρ_h, for a stationary regionalised variable 62
2.16 Commonly used model semivariograms with C_0 set to zero 63
2.17 Different forms of a soil parameter, *v*, with depth, *z* 74
2.18 Examples of variance functions 81
2.19 Spatial variability model of $\bar{s}_u$ at borehole A1 89
2.20 Procedure for estimating the random measurement component from the ACVF 91
2.21 Procedure for estimating the random measurement component from the ACF 91
2.22 Estimation technique proposed by Kulatilake and Southworth (1987) 94

Chapter 3. Development of a Micro-Computer Based Data Acquisition System for the Cone Penetration Test

3.1 Fugro Consultants International Pty. Ltd. data acquisition system 103
3.2 Depth box: (a) internal details, (b) attached to drilling rig 106
3.3 Schematic diagram of the microprocessor interface 108
3.4 Micro-computer and microprocessor interface 110
3.5 Flowchart of the microprocessor interface software, *CPTRead* 111
3.6 An example of the *CPTest* screen 114

3.7 An example of a screen plot produced by *CPTView* 116
3.8 An example of a graphical plot produced by *CPTPlot* 117
3.9 An example of a data table produced by *CPTPlot* 118
3.10 An example of an unrationalised graphical plot produced by *CPTPlot* 120
3.11 Flowchart of the University of Adelaide CPT data acquisition system..... 122
3.12 Depth box calibration curve 124
3.13 Cone penetrometer calibration curve - cone tip resistance 125
3.14 Cone penetrometer calibration curve - sleeve friction 126
3.15 An example of q_c and f_s *falling-off* at rod changes and *noise spikes* 128

Chapter 4. Experimental Programme

4.1 Location of field study site..... 133
4.2 Initial layout of field testing 134
4.3 Referencing system used for the one metre, laterally spaced CPTs 135
4.4 Edson drilling rig 136
4.5 Proline drilling rig..... 137
4.6 Toyota 4WD drilling rig 137
4.7 Amended testing layout 140
4.8 Graphical representation of borehole logs. Contours to surface of: (a) Calcareous Mantle; (b) Limy Surficial Layer; (c) Keswick Clay, to AHD; and (d) 3D representation. 142
4.9 Maximum and minimum daily temperatures for the Adelaide city area for 1992 and 1993..... 144
4.10 Average daily relative humidity for the Adelaide city area for 1992 and 1993 144
4.11 Daily rainfall for the Adelaide city area for 1992 and 1993 145
4.12 Daily evaporation for the Adelaide city area for 1992 and 1993..... 145
4.13 Maximum and minimum daily temperatures for the Adelaide city area for 3rd July - 14th August 1992 and 16th February - 4th March 1993..... 146
4.14 Average daily relative humidity for the Adelaide city area for 3rd July - 14th August 1992 and 16th February - 4th March 1993 146
4.15 Daily rainfall for the Adelaide city area for 3rd July - 14th August 1992 and 16th February - 4th March 1993..... 147
4.16 Daily evaporation for the Adelaide city area for 3rd July - 14th August 1992 and 16th February - 4th March 1993..... 147
4.17 Contour plot of South Parklands site 148
4.18 3-dimensional surface plot of South Parklands site..... 149
4.19 Location of site for horizontal spatial variability field study..... 150
4.20 Trailer mounted CPT equipment for testing in the horizontal direction..... 151
4.21 Layout of steel lateral restraint piers 152
4.22 Depth box arrangement used to measure horizontal penetration depths..... 153

4.23 Results of the horizontal CPT at Keswick 154
4.24 Locations of additional CPTs performed in the determination of N_k 156
4.25 Variation of N_k with undrained shear strength, s_u 159
4.26 Locations of tests performed by Do & Potter (1992) and van Holst Pellekaan & Cathro (1993) 160
4.27 Variation of N_k with undrained shear strength, s_u, including results from Do & Potter (1992) and van Holst Pellekaan & Cathro (1993).....161
4.28 Values of N_k determined from Equation (2.5) compared with those obtained by Teh and Houlsby (1991) 162
4.29 Values of N_k determined from Equation (2.5) compared with those obtained by Teh and Houlsby (1991) including results from Do & Potter (1992) and van Holst Pellekaan & Cathro (1993).....163
4.30 Measured values of s_u compared with s_u^* predicted by Equation (2.7) from Baligh (1975).....164
4.31 Measured values of s_u compared with s_u^* predicted by Equation (2.8) from Keaveny and Mitchell (1986) 164
4.32 Measured values of s_u compared with s_u^* predicted by Equation (2.9) from Teh and Houlsby (1991) 165
4.33 Measured values of s_u compared with s_u^* predicted by Equation (2.10) from Teh and Houlsby (1991) 165

Chapter 5. Examination of the Small-Scale Spatial Variability of the Keswick Clay

5.1 Comparison of semivariogram output by *SemiAuto* with that given by Clark (1979).....169
5.2 A typical screen from *SemiAuto* 170
5.3 A typical screen from the program *Monte*.....171
5.4 Envelope of maxima and minima of measurements of q_c from all CPTs performed at the South Parklands site, except for CD1 to CD50 173
5.5 Envelope of maxima and minima of measurements of q_c from CPTs CD1 to CD50 performed at the South Parklands site.....174
5.6 Histograms of measurements of q_c from all CPTs performed at the South Parklands site.....174
5.7 Measured cone tip resistance, q_c, for sounding C8 177
5.8 Measured cone tip resistance, q_c, within Keswick Clay for sounding C8.....177
5.9 Residuals of q_c, for sounding C8, after removing the quadratic trend.....178
5.10 Sample and model ACFs obtained from the residuals of q_c for C8.....179
5.11 Sample ACF, showing Bartlett's limits, obtained from the residuals of q_c for sounding C8, and used to evaluate Bartlett's distance 180
5.12 Relationship between the scale of fluctuation, δ_V, and Bartlett's distance, r_B 181

5.13 Experimental and model semivariograms of residual q_c data from C8 185
5.14 Experimental and model semivariograms of residual q_c data from A8 - an example of an *excellent fit* 187
5.15 Experimental and model semivariograms of residual q_c data from CD30 - an example of a *good fit* 187
5.16 Experimental and model semivariograms of residual q_c data from D5 - an example of a *poor fit* 188
5.17 Sample and model ACFs of the residuals of s_u, for C8, obtained by converting measurements of q_c using N_k = 20, and 40 190
5.18 Experimental and model semivariograms of the residuals of s_u, for C8, obtained by converting measurements of q_c using N_k = 20 191
5.19 Experimental and model semivariograms of the residuals of s_u, for C8, obtained by converting measurements of q_c using N_k = 40 191
5.20 Horizontal spatial variability data along transect A5 to K5 193
5.21 Sample ACFs of the residuals of the horizontal spatial variability data for transect A5 to K5 194
5.22 Experimental semivariograms of the residuals of the horizontal spatial variability data for transect A5 to K5 194
5.23 Experimental semivariogram of the residuals of transect A5 to K5, at a depth of 3.5 metres 195
5.24 Horizontal spatial variability data along transect CD1 to CD50 196
5.25 Sample ACFs of the residuals of the horizontal spatial variability data for transect CD1 to CD50 198
5.26 Experimental semivariograms of the residuals of the horizontal spatial variability data for transect CD1 to CD50 198
5.27 Experimental semivariogram of the residuals of transect CD1 to CD50 at a depth of 3.5 metres 199
5.28 Horizontal spatial variability data, along transect CD1 to CD50, averaged over depths 3.5 m to 4.5 m below the ground surface 200
5.29 Sample ACF of the residuals of the data, for transect CD1 to CD50, averaged over depths 3.5 m to 4.5 m below the ground surface 201
5.30 Experimental semivariogram of the residuals of the data, for transect CD1 to CD50, averaged over depths 3.5 m to 4.5 m below the ground surface 201
5.31 Horizontal CPT data with quadratic trend function 202
5.32 Residuals of the horizontal CPT data after quadratic trend removal 203
5.33 Sample and model autocorrelation functions of the de-trended horizontal CPT data 204
5.34 Experimental and model semivariograms of the de-trended horizontal CPT data 205
5.35 Scales of spatial variability modelling in geotechnical engineering 206

5.36 The two spherical semivariogram models used to describe the horizontal spatial variability of the Keswick Clay 209
5.37 Nested horizontal spatial variability model for Keswick Clay 210
5.38 Relationship between δ_v and a, OLS best fit linear function 211
5.39 Relationship between δ_v and a, OLS best fit power function 212
5.40 Relationship between r_B and a, OLS best fit power function 212
5.41 Sleeve friction measurements from A0 214
5.42 Sleeve friction measurements from horizontal CPT performed at the Keswick site 214
5.43 Rebound phenomenon from A0 215
5.44 Rebound phenomenon from the horizontal CPT from the Keswick site 215
5.45 Sleeve friction measurements from CPTs performed in red-brown earth and estuarine sands and clays 216
5.46 Sleeve friction measurements from I1 217
5.47 Residuals of sleeve friction measurements from I1 217
5.48 Sample autocorrelation function and model obtained from residuals of f_s measurements from I1 218
5.49 Experimental semivariogram and spherical model obtained from residuals of f_s measurements from I1 219
5.50 Sample cross-correlation function of cone tip resistance and sleeve friction measurements, from within the Keswick Clay, from CPT I1 221
5.51 Sample CCF of q_c and f_s measurements from CPT A3 223
5.52 Sample CCF of q_c and f_s measurements from CPT B10 223
5.53 Sample CCF of q_c and f_s measurements from CPT: (a) A1, and (b) CD40 224
5.54 Sample CCF of q_c and f_s measurements from the horizontal CPT performed at the Keswick site 225
5.55 Extent of the failure zone of the CPT in Keswick Clay 228
5.56 Data from borehole A-1 with models proposed by Asaoka and A-Grivas (1982) and Ravi (1992) 230
5.57 Data from borehole A-1 with the model proposed by Ravi (1992) and that obtained by using rescaled residuals 233
5.58 Sample PACF obtained from the residuals of q_c for C8 after classical transformation, that is, removal of the OLS quadratic trend 234
5.59 Rescaled residuals after fitting an AR(3) model to the classically transformed measurements of q_c for sounding C8 236
5.60 ACF of the rescaled residuals of q_c for C8 after fitting an AR(3) model 236
5.61 Measured q_c data from C8 with the AR(3) model obtained by using rescaled residuals 237
5.62 Residuals of q_c, for sounding C8, after first-differencing 237

5.63 Sample ACF obtained from the residuals of q_c, for sounding C8, after first-differencing 238
5.64 Experimental semivariogram obtained from the residuals of q_c, for sounding C8, after first-differencing 239
5.65 Sample PACF obtained from the residuals of q_c, for sounding C8, after first-differencing 239
5.66 Rescaled residuals, after fitting an IMA(1,1) model to the first-differenced measurements of q_c, for sounding C8 240
5.67 ACF of the rescaled residuals of q_c for C8 after fitting an IMA(1,1) model 241
5.68 Measured q_c data from C8 with the IMA(1,1) model obtained by using rescaled residuals 241
5.69 Measured q_c data from horizontal CPT, from the Keswick site, with the AR(6) model obtained by using rescaled residuals 246
5.70 Measured q_c data from horizontal CPT, from the Keswick site, with the ARIMA(3,1,3) model obtained by using rescaled residuals 247
5.71 Forecasts of q_c measurements obtained from classically transformed data, AR(3), and first-differenced data, IMA(1,1), for C8 248
5.72 Forecasts of q_c measurements obtained from classically transformed data, AR(6), and first-differenced data, ARIMA(3,1,3), for the horizontal CPT 249
5.73 Five random realisations of the AR(3) process for CPT C8 obtained from *Monte* 251
5.74 Envelope of 1,000 realisations of the AR(3) process, for CPT C8, obtained from *Monte* 252
5.75 Envelope of 1,000 realisations of the IMA(1,1) process, for CPT C8, obtained from *Monte* 252
5.76 Envelope of 1,000 realisations of the AR(6) process, for the horizontal CPT, obtained from *Monte* 253
5.77 Envelope of 1,000 realisations of the ARIMA(3,1,3) process, for the horizontal CPT, obtained from *Monte* 254
5.78 Results of one-step ahead ordinary kriging of C8 from *OKB2D* 256
5.79 Results of one-step ahead ordinary kriging of the horizontal CPT using *OKB2D* 256
5.80 Results of ordinary kriging using 200 mm spaced input data from C8 261
5.81 Results of ordinary kriging using 200 mm spaced input data from the horizontal CPT 261
5.82 Ordinary kriged estimates and the 95% confidence limits ($\pm 2\sigma$) using 200 mm spaced input data from C8 262
5.83 Ordinary kriged estimates and the 95% confidence limits ($\pm 2\sigma$) using 200 mm spaced input data from the horizontal CPT 262
5.84 Ordinary kriged forecasts at 5 mm intervals for C8 264

5.85 Ordinary kriged forecasts at 5 mm intervals for the horizontal CPT 264
5.86 Sample ACFs after: (a) no trend removal; and (b) a linear trend removal 271
5.87 Sample ACFs for: (a) 50 mm spaced data set; and (b) 200 mm spaced data set 273
5.88 Sample ACFs for: (a) 20 mm spaced data set; and (b) 100 mm spaced data set 276

Chapter 6. Compilation of a Data Base of Geotechnical Properties of the Keswick and Hindmarsh Clays

6.1 Location of boreholes included in *KESWICK* 287
6.2 Procedure used to determine the three-dimensional coordinates for each test in the *KESWICK* data base 290
6.3 Three-dimensional coordinates associated with each test in *KESWICK* 290
6.4 Variation of the depth below ground of the surface of the Keswick Clay 293
6.5 Variation of the depth below ground of the surface of the Hindmarsh Clay Sand Member 293
6.6 Variation of the depth below ground of the surface of the Hindmarsh Clay Layer 295
6.7 Variation of the surface of the Keswick Clay to the AHD 295
6.8 Variation of the surface of the Hindmarsh Clay Sand Member to theAHD 297
6.9 Variation of the surface of the Hindmarsh Clay Layer to the AHD 297
6.10 Relationship between moisture content and the depth below ground for the Keswick Clay, undifferentiated Keswick Clay-Hindmarsh Clay, and the Hindmarsh Clay Layer 299
6.11 Relationship between dry density and the depth below ground for the Keswick Clay, undifferentiated Keswick Clay-Hindmarsh Clay, and the Hindmarsh Clay Layer 299
6.12 Relationship between w, ρ_d, and S_r for Keswick Clay with $G_s = 2.70$ 301
6.13 Relationship between w, ρ_d, and S_r for Keswick Clay with $G_s = 2.75$ 302
6.14 Relationship between w, ρ_d, and S_r for undifferentiated Keswick Clay-Hindmarsh Clay with $G_s = 2.75$ 303
6.15 Relationship between w, ρ_d, and S_r for the Hindmarsh Clay Layer with $G_s = 2.77$ 304
6.16 Relationship between S_r and depth below ground for Keswick Clay with $G_s = 2.75$ 304
6.17 Undrained shear strength, s_u, of the Keswick Clay obtained from the first stage of UU tests 306
6.18 Undrained shear strength, s_u, of undifferentiated Keswick Clay-Hindmarsh Clay obtained from the first stage of UU tests 306

6.19 Undrained shear strength, s_u, of the Hindmarsh Clay Sand Member obtained from the first stage of UU tests 307
6.20 Undrained shear strength, s_u, of the Hindmarsh Clay Layer obtained from the first stage of UU tests 307
6.21 Histograms of the undrained shear strength, s_u, of the Keswick Clay, undifferentiated Keswick Clay-Hindmarsh Clay and the Hindmarsh Clay Layer obtained from the first stage of UU tests 308
6.22 Relationship between s_u and depth below ground for the Keswick Clay, undifferentiated Keswick Clay-Hindmarsh Clay and the Hindmarsh Clay Layer obtained from several in situ tests 309
6.23 Relationship between s_u and w for the Keswick Clay, undifferentiated Keswick Clay-Hindmarsh Clay, and the Hindmarsh Clay Layer obtained from the first stage of UU tests 309
6.24 Relationship between s_u and ρ_d for the Keswick Clay, undifferentiated Keswick Clay-Hindmarsh Clay and the Hindmarsh Clay Layer obtained from the first stage of UU tests 310
6.25 Relationship between s_u and σ_3 for the Keswick Clay, undifferentiated Keswick Clay-Hindmarsh Clay and the Hindmarsh Clay Layer obtained from the first stage of UU tests 311
6.26 Relationship between s_u/σ_{v0} and depth below ground for the Keswick Clay, undifferentiated Keswick Clay-Hindmarsh Clay and the Hindmarsh Clay Layer obtained from the first stage of UU tests 311
6.27 Relationship between s_u and σ_3 for the Hindmarsh Clay Sand Member obtained from up to three stages of UU tests 312
6.28 Relationship between E_u and depth below ground for the Keswick Clay, undifferentiated Keswick Clay-Hindmarsh Clay and the Hindmarsh Clay obtained from the first stage of UU tests 313
6.29 Histograms of E_u of the Keswick Clay, undifferentiated Keswick Clay-Hindmarsh Clay and the Hindmarsh Clay Layer obtained from the first stage of UU tests 314
6.30 Relationship between E_u and depth below ground for the Keswick Clay, undifferentiated Keswick Clay-Hindmarsh Clay and the Hindmarsh Clay Layer obtained from a number of in situ tests 314
6.31 Relationship between E_u/σ_{v0} and depth below ground for the Keswick Clay, undifferentiated Keswick Clay-Hindmarsh Clay and the Hindmarsh Clay Layer obtained from up to three stages of UU tests 316
6.32 Relationship between SPT Number, N, measured in the Hindmarsh Clay Sand Member and the depth below the surface of this layer 316

6.33 Relationship between total soil suction, *u*, and moisture content, *w*, for the Keswick Clay, undifferentiated Keswick Clay-Hindmarsh Clay and the Hindmarsh Clay Layer 318
6.34 Relationship between total soil suction and depth below ground for: (a) summer; (b) autumn; (c) winter; and (d) spring 319
6.35 Contours of s_u for Keswick Clay based on the results of unconsolidated undrained triaxial tests using an averaging process based on pile design 321
6.36 Contours of s_u for Keswick Clay based on the results of unconsolidated undrained triaxial tests using an averaging process based on raft design 321

Chapter 7. Examination of the Large-Scale Lateral Spatial Variability of the Keswick Clay

7.1 Locations of the spatially averaged s_u observations from the *0 to 3 metre* data set used in the large-scale spatial variability analyses 328
7.2 Second-degree polynomial trend surface of s_u (kPa) obtained by least squares regression of the *0 to 3 metre* data set using *S-PLUS for Windows* 329
7.3 Convention used by *Vario* to calculate the semivariogram 330
7.4 North-South and East-West experimental semivariograms, with associated spherical model, of the detrended *0 to 3 metre* data set 330
7.5 Number of pairs associated with the North-South and East-West experimental semivariograms of the detrended *0 to 3 metre* data set 331
7.6 Omnidirectional experimental semivariogram, with associated spherical model, of the detrended *0 to 3 metre* data set 332
7.7 Number of pairs associated with the omnidirectional experimental semivariogram of the detrended *0 to 3 metre* data set 333
7.8 The three semivariogram models which describe the spatial variability of the undrained shear strength of the Keswick Clay 334
7.9 Nested model semivariogram of the spatial variability of the undrained shear strength of the Keswick Clay 335
7.10 Map of the residuals obtained from the cross validation of the *0 to 3 metre* data set 337
7.11 Scatterplot of the residuals obtained from the cross validation of the *0 to 3 metre* data set 338
7.12 Locations of the additional data used to obtain kriged estimates 340
7.13 The spatial variation of $\bar{s}_u$ of Keswick Clay, within a depth of 3 metres below its surface, as given by ordinary kriging 345
7.14 The variation of the kriging standard deviation, σ_k, associated with the estimates given in Figure 7.13 345
7.15 The spatial variation of $\bar{s}_u$ of Keswick Clay, within a depth of 3 metres below its surface, as given by polygonal estimation via *DeltaGraph* 347

Chapter 8. Significance of Spatial Variability with Respect to Geotechnical Engineering Design

8.1 Keswick Clay embankment analysed using *PROBSN* 350
8.2 Influence of the scale of fluctuation, δ_v, on the probability of slope failure, P_f .. 351
8.3 The procedure used to calculate q_{ca} 354
8.4 CPTs adjacent to F5 356
8.5 Data from the 6 CPTs adjacent to F5, including their mean 357
8.6 Relationship between the percentage error of Q_A and the radial distance of the CPT, used to determine the pile at F5, using $q_{si(max)}$ = 35 kPa 358
8.7 Relationship between the percentage error of Q_A and the radial distance of the CPT, used to determine the pile at F5, using $q_{si(max)}$ = 80 kPa 359
8.8 Relationship between the percentage error of Q_A and the radial distance of the CPT, used to determine the pile at F5, using an unlimited $q_{si(max)}$ 360
8.9 Plan view of the grid layout used for the simulated 3D data 362
8.10 Isometric view of the grid layout used for the simulated 3D data 363
8.11 A typical screen from *LCPCSim* 366
8.12 Experimental semivariograms for simulated data, compared with the model semivariogram for a = 0.2 metres 367
8.13 Experimental semivariograms for simulated data, compared with the model semivariogram for a = 1.0 metres 367
8.14 Relationship between the range, a, and the maximum and minimum percentage errors, E_{Q_A}, assuming the pile is exclusively founded within the Keswick Clay, and using 100 simulations at each range 369
8.15 Relationship between the range, a, and the maximum and minimum percentage errors, E_{Q_A}, assuming the pile is founded within soils similar to those encountered at the South Parklands site, and using 100 simulations at each range 369

Appendix A Selected Cone Penetration Test Results from Field Study

A.1 Cone penetration test results from sounding A0 399
A.2 Cone penetration test results from sounding A1 400
A.3 Cone penetration test results from sounding A2 401
A.4 Cone penetration test results from sounding A4 402
A.5 Cone penetration test results from sounding A6 403
A.6 Cone penetration test results from sounding A8 404
A.7 Cone penetration test results from sounding A10 405
A.8 Cone penetration test results from sounding B1 406
A.9 Cone penetration test results from sounding B5 407
A.10 Cone penetration test results from sounding B8 408
A.11 Cone penetration test results from sounding C0 409

A.12 Cone penetration test results from sounding C4.....410
A.13 Cone penetration test results from sounding C8.....411
A.14 Cone penetration test data from sounding C8 (1 of 13) 412
A.15 Cone penetration test data from sounding C8 (2 of 13) 413
A.16 Cone penetration test data from sounding C8 (3 of 13) 414
A.17 Cone penetration test data from sounding C8 (4 of 13) 415
A.18 Cone penetration test data from sounding C8 (5 of 13) 416
A.19 Cone penetration test data from sounding C8 (6 of 13) 417
A.20 Cone penetration test data from sounding C8 (7 of 13) 418
A.21 Cone penetration test data from sounding C8 (8 of 13) 419
A.22 Cone penetration test data from sounding C8 (9 of 13) 420
A.23 Cone penetration test data from sounding C8 (10 of 13).....421
A.24 Cone penetration test data from sounding C8 (11 of 13).....422
A.25 Cone penetration test data from sounding C8 (12 of 13).....423
A.26 Cone penetration test data from sounding C8 (13 of 13).....424
A.27 Cone penetration test results from sounding C10.....425
A.28 Cone penetration test results from sounding CD1.....426
A.29 Cone penetration test results from sounding CD30.....427
A.30 Cone penetration test results from sounding CD40.....428
A.31 Cone penetration test results from sounding D5 429
A.32 Cone penetration test results from sounding D8 430
A.33 Cone penetration test results from sounding E1.....431
A.34 Cone penetration test results from sounding E7.....432
A.35 Cone penetration test results from sounding G0 433
A.36 Cone penetration test results from sounding G5 434
A.37 Cone penetration test results from sounding G10 435
A.38 Cone penetration test results from sounding H7 436
A.39 Cone penetration test results from sounding H10 437
A.40 Cone penetration test results from sounding I1.....438
A.41 Cone penetration test results from sounding I9.....439
A.42 Cone penetration test results from sounding J8.....440
A.43 Cone penetration test results from sounding K0 441
A.44 Cone penetration test results from sounding K10 442

List of Tables

Chapter 2. Literature Review

2.1 Summary of stratigraphic units underlying the Adelaide city area 11
2.2 Summary of Atterberg limit tests 18
2.3 Summary of Atterberg limit tests 18
2.4 Some of the variables which influence N_k 31
2.5 Variables contributing to CPT equipment error 36
2.6 Variables contributing to operator/procedural errors 38
2.7 Commonly used model semivariograms 63
2.8 Summary of statistical properties 75
2.9 Theoretical autocorrelation functions used to determine the scale of fluctuation, δ_v 83
2.10 Autocorrelation functions, correlation distances and scales of fluctuations given by various researchers 85-87
2.11 Relationship between the scale of fluctuation, δ_v, and the correlation distance, v_o, for various ACF models 88
2.12 Model semivariograms and their parameters as given by various researchers 99

Chapter 3. Development of a Micro-Computer Based Data Acquisition System for the Cone Penetration Test

3.1 Data conversion factors 112
3.2 Relationships used to calculate data conversion factors 113

Chapter 4. Experimental Programme

4.1 Cone penetration testing programme 139
4.2 Summary of borehole logs 141
4.3 Summary of unconsolidated undrained triaxial tests 156
4.4 Summary of additional CPT results and calculated values of N_k 157
4.5 Undrained shear strengths, s_u^*, predicted from values of N_k determined from Equations (2.5) and (2.7) to (2.10) 163

Chapter 5. Examination of the Small-Scale Spatial Variability of the Keswick Clay

5.1 Global statistics of measurements of q_c from all CPTs performed at the South Parklands site 172

5.2 Interpolated depths below ground to the surface of the Keswick Clay, relevant to the CPTs performed at the South Parklands Site 175
5.3 Results of random field theory analyses on detrended residuals of q_c measurements obtained from 30 of the 222 vertical CPTs at the South Parklands site 182
5.4 Results of the runs tests and Kendall's τ tests performed on detrended residuals of q_c measurements obtained from 30 of the 222 vertical CPTs at the South Parklands site 184
5.5 Results of geostatistical analyses performed on measurements of q_c obtained from 30 of the 222 vertical CPTs at the South Parklands site 186
5.6 Measurements of q_c from vertical CPTs A5 to K5 used to generate horizontal spatial variability data 193
5.7 Results of random field theory and geostatistical analyses of horizontal spatial variability data, from transect A5 to K5, at various depths 195
5.8 Results of random field theory and geostatistical analyses of horizontal spatial variability data, from transect CD1 to CD50, at various depths 197
5.9 Summary of random field theory analyses, performed on the residuals of the horizontal CPT data, obtained from the Keswick site 203
5.10 Results of cross-correlation analyses performed on measurements of q_c and f_s, from 60 of the 222 vertical CPTs, from the South Parklands site 222
5.11 Summary of vertical and horizontal correlation distances ($\equiv \delta_v$) of s_u, q_c and f_s of clay soils published in the literature 227
5.12 Undrained shear strength data from borehole A-1 presented by Asaoka and A-Grivas (1982) and re-examined by Ravi (1992) 231
5.13 Results of random field analyses performed on classically transformed residuals of q_c measurements obtained from 30 of the 222 vertical CPTs performed at the South Parklands site 243
5.14 Results of random field analyses performed on first-differenced residuals of q_c measurements obtained from 30 of the 222 vertical CPTs performed at the South Parklands site 244
5.15 First 10 forecasts of q_c (MPa) for CPT C8 248
5.16 First 10 forecasts of q_c (MPa) for the horizontal CPT from the Keswick site 250
5.17 Results of one-step ahead ordinary kriging from *OKB2D* 255
5.18 Results of one-step ahead ordinary kriging from *OKB2D*, compared with those obtained from random field analyses 257
5.19 Results of forecasts at 5 mm spacings obtained by ordinary kriging using *OKB2D* 260
5.20 Comparison of the sum of the squared differences, *SSD*, (MPa^2) between linear interpolation and ordinary kriging of C8 and the horizontal CPT 260

5.21 Results of forecasts obtained by ordinary kriging, using *OKB2D*, compared with those obtained from random field theory 263
5.22 Summary of trend removal analyses (vertical spatial variability - C8)..... 270
5.23 Summary of sample spacing analyses (vertical spatial variability - C8)..... 272
5.24 Summary of trend removal analyses (horizontal spatial variability) 275
5.25 Summary of sample spacing analyses (horizontal spatial variability)..... 277

Chapter 6. Compilation of a Data Base of Geotechnical Properties of the Keswick and Hindmarsh Clays

6.1 Information stored in *GEOSHARE* 283
6.2 Statistics associated with w and ρ_d of the various soil layers stored in *KESWICK* 300
6.3 Statistics associated with s_u (kPa) obtained from UU tests..... 305
6.4 Statistics associated with E_u (MPa) obtained from UU tests 313
6.5 Statistics associated with E_u (MPa) obtained from SPLT and SBPTs 315

Chapter 7. Examination of the Large-Scale Lateral Spatial Variability of the Keswick Clay

7.1 Summary statistics of the results of cross validation analyses compared with the original data 337
7.2 Summary of additional $\bar{s}_u$ data from UU tests on Keswick Clay, used to assess the spatial variability model and estimation procedure..... 339
7.3 Summary of results of ordinary kriged estimates from *Krige* using original non-detrended data 341
7.4 Summary of results of ordinary kriged estimates from *Krige* using detrended data 341
7.5 Summary of results of estimates of $\bar{s}_u^*$ (kPa) and sum of the squared differences, *SSD*, (kPa^2) from polygonal, inverse distance and inverse distance squared estimation regimes..... 343

Chapter 8. Significance of Spatial Variability with Respect to Geotechnical Engineering Design

8.1 Global statistics of measurements of q_c within the Keswick Clay, as well as all soils encountered at the South Parklands site..... 364

Appendix C Data Base of the Geotechnical Properties of the Keswick and Hindmarsh Clays

C.1 Data from Coffey Partners International Pty. Ltd. 455
C.2 Data from Rust PPK Consultants Pty. Ltd. 457
C.3 Data from SACON 459

C.4 Data from Golder Associates Pty. Ltd.
(formerly Woodburn Fitzhardinge Geotechnical).....461
C.5 Data from ACER Wargon Chapman Pty. Ltd.
(formerly Hosking Oborn Freeman and Fox).....463
C.6 Data from Koukourou and Partners 465
C.7 Data from Connell Wagner (SA) Pty. Ltd.....467
C.8 Data from Kinhill Engineers Pty. Ltd.....469

Notation

Throughout the thesis, the following terms refer to the properties presented below. Abbreviations and additional descriptions are given in the Glossary.

A_b; A_{cn}; A_s	area of the base of the cone, usually 1000 mm^2 = $\frac{\pi D^2}{4}$; net area ratio of the cone = $\frac{d_o^2}{D^2}$; surface area of the friction sleeve;
A_p	area of the base of a pile;
a	range of influence - the distance at which samples become independent of one another;
a_c	radius of the electric cone penetrometer;
a_t	random component, or *shock*, used in ARMA models with a mean of zero and a variance equal to σ_a^2;
B	backshift operator;
C	a parameter, when added to C_0, represents the *sill* of a transitive type of semivariogram;
C_p	circumference of the shaft of a pile;
CV	coefficient of variation = $\frac{\sigma}{m} \times 100\%$;
C_{XY}	covariance between data sets X and Y;
C_0	nugget effect - arises from the regionalised variable being so erratic over a short distance that the semivariogram goes from zero to the level of the nugget in a distance less than the sampling interval;
$\frac{C_0}{C+C_0}$	relative nugget;

c parameter used in Kendall's τ test, where the probability of concordance is c times as large as the probability of discordance;

c_k; c_k^* autocovariance at lag k; sample autocovariance at lag k;

$c_{k_{XY}}$; $c^*_{k_{XY}}$ cross-covariance coefficient between time series X and Y at lag k; sample cross-covariance coefficient at lag k;

c_u; c' undrained and drained cohesion intercept;

c_v coefficient of consolidation;

D diameter of the base of the cone, usually 35.7 mm;

D_p the width of a pile, or in the case of a circular cross-section pile, its diameter;

D_{50} diameter of the grain for which 50% of the particles in the sample are finer, by weight;

d_i distance from the estimation point to the ith neighbour (used in inverse distance and inverse distance squared weightings);

d_o smallest diameter of the cone at the o-ring seal;

$\bar{d}_v$ is the average distance between the intersections of the fluctuating property, $v(z)$, and its mean, $\bar{v}$;

E[...] expected value, or mean;

E; E_u; $E_{u(50)}$ Young's modulus of elasticity; undrained Young's modulus of elasticity; undrained Young's modulus of elasticity given by the secant modulus at 50% of the peak axial strain;

E_{Q_A} percentage error between the 'true' Q_A and that based on measurements;

E^+; E^- Young's modulus of elasticity at peak shear strength on the increasing portion of the stress/strain curve and the decreasing portion of the stress/strain curve;

e void ratio;

e_t random testing error term in an ARMA model as proposed by Wu and El-Jandali (1985);

F_c; F_s total force acting on the cone tip and the friction sleeve;

F_R friction ratio = $\frac{f_s}{q_c} \times 100\%$;

FoS factor of safety = $\frac{\text{Forces } \mathbf{resisting} \text{ instability}}{\text{Forces } \mathbf{causing} \text{ instability}}$;

f initial shear stress ratio = $\frac{\sigma_{v0} - \sigma_{h0}}{2s_u}$;

f_s sleeve friction, as measured by the cone penetration test;

G shear modulus;

G_s specific gravity of solids;

h the displacement between data pairs;

I_P plasticity index = $w_L - w_P$;

I_{pt} instability index;

I_r rigidity index = $\frac{G}{s_u} = \frac{E_u}{3s_u}$;

K the maximum number of lags, k, that r_k and r_{kk} should not be calculated beyond;

$K_1(x)$ modified Bessel function of the second kind and first order;

K_0 coefficient of earth pressure at rest; that is, at zero lateral strain;

k lag;

k_c penetrometer bearing capacity factor;

L_p length of a pile;

m mean, or average value;

m_{v_x} measurement of the parameter, v_x;

N_k; $\overline{N}_k$ cone factor; average cone factor (note that k does not refer to lag);

n number of observations, or data, in a data set;

n_1; n_2; n_3 number of observations greater than the mean, less than the mean, and equal to the mean, respectively, as used in the runs test;

n_p number of parameters that must be estimated in the model under consideration, and which equals p - q, where p, q are the number of AR and MA terms, respectively;

OCR overconsolidation ratio;

P_f probability of failure;

PRE percentage random testing error as proposed by Wu and El-Jandali (1985);

p mean normal stress;

Q Box-Pierce chi-square statistic;

Q_A; Q_A^* allowable axial capacity of a statically loaded pile; estimate of the allowable axial capacity of a statically loaded pile based on measurements;

Q_B; Q_S axial capacity of the base, and shaft, of a statically-loaded pile;

Q_U ultimate axial capacity of a statically loaded pile;

q lag number at which ρ_k is thought to be equal to zero;

q_c; $\bar{q}_c$; q_t cone tip resistance, as measured by the cone penetration test; average of the measured values of cone tip resistance over the length of the triaxial specimen; cone tip resistance corrected for the influence hydrostatic pressures acting on the notched section of the cone;

q_{ca}; q'_{ca} clipped average cone tip resistance and intermediate clipped average cone tip resistance, at the level of the pile base (kPa);

$q_{si(max)}$ limit unit skin friction of the ith soil layer;

R number of runs used in the runs test;

RAW An irrigation/soil science parameter which measures the water reservoir of the soil between full point, –8 kPa, and refill point, –60 kPa, and is expressed in mm (Brooker et al., 1995);

RD relative density of sands;

R_t residuals used in the *significance test on trends* method for assessing stationarity;

R_{q_c} residuals, or the difference between measurements of q_c and the trend function obtained by the method of OLS;

R_0 the ACF nugget: the difference between unity and the value of the autocorrelation coefficient at lag zero, r_0, obtained by extrapolating the sample ACF back to lag zero;

r; r^2 correlation coefficient; coefficient of determination;

r_B Bartlett's distance; that is, the distance at which the sample ACF intersects the limit obtained from Bartlett's formula;

r_k; r_k sample autocorrelation at lag k; autocorrelation at lag k of residuals;

r_{kk} sample partial autocorrelation coefficient at lag k;

$r_{k_{XY}}$ sample cross-correlation coefficient between time series X and Y at lag k;

r_p the radial distance of the plastic boundary from the axis of penetration measured at a large enough distance above the cone penetrometer tip;

S the difference between the number of concordant pairs and the number of disconcordant pairs (used in Kendall's τ test);

S_i the ith sample;

S_r degree of saturation;

SSD sum of the squared differences = $\sum_{i=1}^{n}\left(Y_i - Y_i^*\right)^2$. The lower the value of SSD, the better the estimate;

s_u; s_u^*; $\bar{s}_u$ undrained shear strength; estimated undrained shear strength; average undrained shear strength;

s_X sample standard deviation of time series X;

t_i thickness of the ith soil layer;

t_t trend component of a random field;

U	a point, line, area, or block;
u	total soil suction;
u_k	standardised random variable at location k, with properties of zero mean, and standard deviation of unity;
u_{bt}	porewater pressure at the depth of q_c measurements;
V	a block or domain of some volume;
v_k; v_k^*	soil property, v, at point k in a soil mass; measurement of soil property, v, at point k in a soil mass;
v_o	correlation distance of some property, v;
$\hat{W}_t$; $\hat{W}_t^{(r)}$	one-step prediction errors, or residuals; rescaled residuals;
w	moisture content;
w_i	weight applied to the ith sample;
w_L; w_P	liquid limit; plastic limit;
X_i	the value of the property, X, at location, i;
X_t	a time series, or a random field;
Y_t; $\hat{Y}_t$	a time series, or a random field; best linear mean-square predictor of Y_t based on the observations up to distance, $t-1$;
z; z_k	depth of the electric cone penetrometer; depth of the soil property at point k;
z_p	the distance between the cone tip and the plastic boundary measured along the axis of the cone penetrometer;
z_R; z_τ	a parameter used in the runs test and Kendall's τ test, respectively, which is normally distributed, with zero mean and unit variance;
α	a constant used in the variance function, ACF, and semivariogram models, and is known as the *absolute dispersion* in the de Wijsian semivariogram model;

α_f; α_s roughness factor of the cone face = $\frac{\sqrt{3}}{2}\frac{\tau_f}{s_u}$ and cone shaft = $\frac{\sqrt{3}}{2}\frac{\tau_s}{s_u}$;

$\Gamma(n)$ variance reduction factor;

γ; γ_d; γ_{sat} bulk unit weight; dry unit weight; saturated unit weight;

γ_h; γ_h^* semivariogram function at separation distance h; experimental semivariogram, at h, which is based on the sampled data set;

Δu change in total suction;

Δz_0 sampling interval;

δ_H; δ_V scale of fluctuation in the horizontal, and vertical, directions;

δ_v scale of fluctuation of the soil property, v;

δ_{V_2}; δ_{V_3} scale of fluctuation obtained by fitting Vanmarcke's simple exponential, and squared exponential, model (given in Table 2.9), respectively, to the sample ACF;

ε_v vertical strain;

ε_i; ε_t error terms, or white noise components;

ζ_P standardised normal variate associated with the probability, P; that is, from a normal probability density function with zero mean and a standard deviation of unity;

ζ_x the random measurement error at x;

Θ angle of a slope, or embankment, from the horizontal;

θ_i constants used in a moving average process, where i = 1, 2, ...;

λ a parameter used in the Box-Cox variance transformation;

μ Lagrange multiplier;

ξ_x the random perturbation from the trend at x;

ρ_d; ρ_w dry density; density of water (usually taken as 1000 kg/m^3);

ρ_k autocorrelation at lag k;

$\rho_{k_{XY}}$ cross-correlation coefficient between time series *X* and *Y* at lag *k*;

σ; σ_X standard deviation; standard deviation of data set *X*;

σ_3 cell, or confining, pressure applied in a triaxial test;

σ_a^2 white noise variance of the fitted ARIMA model;

σ_e^2 variance of the random testing error;

σ_{equip}^2 variance of equipment effects;

σ'_h; σ'_v effective horizontal and vertical stress;

σ_{h0}; σ_{v0} total in situ horizontal and vertical overburden stress;

σ_k^2; σ_ε^2 kriging variance; estimation variance;

$\sigma_{measure}^2$ total variance of measurement;

σ'_p effective preconsolidation pressure;

$\sigma_{op/proc}^2$ variance of operator and procedural effects;

σ_{random}^2 variance of random testing effects;

σ_z^2 variance of the observed, or transformed, data;

τ test statistic used in Kendall's τ test;

τ_f; τ_s shear stress on the cone face and the sleeve face;

ϕ; ϕ'; ϕ_u; ϕ_d total internal angle of friction; effective internal angle of friction; undrained and drained internal angle of friction;

ϕ_i constants used in an autoregressive, AR, process, where i = 1, 2, ...;

ϕ_{kk} partial autocorrelation at lag *k*;

ψ a constant used in the LCPC Method which allows for the nature of the soil and the pile construction and placement methods;

$\chi_5^2(z)$ the point on the scale of the chi-square distribution having *z* degrees of freedom such that there is an area of 5% under the curve of this distribution above this point;

∇^k difference operator of order *k*.

Glossary

Note: A term with an asterisk (*) beside it, indicates that the definition was obtained from Olea (1991). A term in *italics* implies a cross-reference to another glossary listed item.

ACF Autocorrelation function;

ACVF Autocovariance function;

A/D converter Analogue to digital converter;

AHD Australian height datum - a standard datum surface, effectively a mean sea level, adopted by the National Mapping Council, to which all vertical control for mapping is referred;

AMG Australian map grid - a standard map grid established by the National Mapping Council of Australia and derived from a Transverse Mercator projection of latitudes and longitudes, the coordinates of which are in metres;

Analogue output Transducer output which is a continuous function of the *measurand* (except as modified by the resolution of the transducer);

AR Autoregressive *time series* model;

ARIMA Integrated autoregressive-moving average *time series* model;

ARMA Autoregressive-moving average *time series* model;

ASCII American Standard Code for Information Interchange;

Autocorrelation, $\mathbf{r}_k$ The relationship between any two *time series* observations separated by a *lag* of *k* units;

Bartlett's distance The distance given by the intersection of the sample *ACF* with *Bartlett's limits*;

Bartlett's limits The limits obtained by substitution into Bartlett's equation; that is, $\pm 1.96/\sqrt{N}$;

Bayesian kriging an enhancement of *indicator kriging* which is used when a small number of observations is available, and when significant experience and knowledge about the phenomenon should be accounted for in the estimation process;

BLUE Best linear unbiased estimator;

CCF Cross-correlation function;

CGA Colour graphics adaptor;

CIRIA Construction Industry Research and Information Association (UK);

CIU Isotropically consolidated, undrained triaxial compression test;

CK_0U Undrained triaxial test where the sample is reconsolidated to in situ K_0 conditions prior to shear;

Correlation distance The extent over which samples exhibit strong correlation. Vanmarcke and Fuleihan (1975) defined it as the distance required for the *ACF* to drop from 1 to e^{-1} (0.3679);

CPT Cone penetration test;

Cross validation* A validation method in which observations are temporarily discarded, one at a time, from a data set of size *n*, and *n* estimates are computed using, at most, the remaining ($n - 1$) measurements;

CSMD Colorado School of Mines borehole dilatometer - an in situ test device which measures the modulus of rigidity of rocks;

Data conversion factor Each *mpb* is multiplied by this to yield the digital equivalent of the measured quantity;

DC Direct current;

Digital output Transducer output which is a stepped function of the *measurand*;

DMT Marchetti flate plate dilatometer;

Drift* A mathematical description of the low frequency, large-scale variation of a regionalised variable, (cf. *trend*); also the deviation, from vertical or horizontal, of the CPT;

DST Direct shear test;

EPROM Erasable programmable read only memory;

Falling off A phenomenon associated with measurements of q_c and f_s that occurs when further rods are added to the drill stem and is indicated by these measurements dropping to zero or values significantly less than that recorded immediately above it (cf. Figure 3.15);

FoS Factor of safety;

Friction reducer Narrow local protuberances outside the surface of the *CPT* push rods, placed above the cone penetrometer tip, and provided to reduce the total friction on the push rods;

Geostatistics A mathematical technique used to estimate properties which are spatially dependent;

Gilgais Dome-type undulations of the upper surface of the Keswick Clay and Hindmarsh Clay Formation;

GLS The regression analysis method of generalised least squares;

Heteroscedasticity Non-constant variance;

Hole effect* A *semivariogram* which is not monotonically increasing and which may reflect periodicities in the *random field*;

Homogeneity The property of a *spatial series* when its characteristics are independent of location. Homogeneity is equivalent to *stationarity*;

Homoscedasticity Constant variance;

Indicator kriging* *Simple kriging* or *ordinary kriging* applied to indicator data (samples which have been transformed into binary numbers) sharing the same threshold;

Interrupt driven measurements The *MPU* immediately processes these measurements as soon as an interrupt signal is received;

ISOPT-1 First International Symposium on Penetration Testing, Orlando, Florida, 1988;

kb kilobytes;

Kriging* A collection of generalised linear regression techniques for minimising an estimation variance defined from a prior model. In contrast to classical linear regression, kriging takes into account stochastic dependence among the data;

Kurt., kurtosis* The kurtosis is a measure of the peakedness of a data distribution around the mode. A kurtosis: equal to 3 suggests a normal, or Gaussian, distribution; < 3 implies a lower concentration near the mean than a normal distribution; and > 3 suggests that the distribution has an excess of values near the mean;

Lag, *k** The difference in the time of occurrence of two events in a *time series*, or in relation to a *spatial series*, the lag is the distance between the locations of two random variables in a *random field*;

LCD Liquid crystal display;

LCPC method A method for determining the axial capacity of a statically loaded pile based on *CPT* data, and developed at the Laboratoire Central des Ponts et Chaussées, France;

LNS The regression analysis method of least normal squares;

Load cell A device, usually consisting of electrical resistance strain gauges, which generates an output signal proportional to the applied force or weight;

MA Moving average *time series* model;

Markov process* A stochastic process in which a prediction is determined solely by the closest *n* observations, and is stochastically independent from all remaining, more distant observations;

Measurand The physical quantity, property, or condition that is to be measured;

Missing depth A *rationalised depth* which has no associated measurement of q_c and/or f_s;

Modulus of sub-grade reaction The elastic modulus of the subgrade which accounts for pavement deformation;

Monte Carlo* methods Any number of procedures that use simulated random samples to make inferences about actual populations;

mpb Microprocessor bit - the digital unit that is multiplied by the data conversion factor to yield the digital equivalent of the measured quantity. (e.g. 1 mpb of f_s measurements is equivalent to 0.488 kPa);

MPU Microprocessor unit - the microchip that forms the core of the microprocessor interface;

NATA National Association of Testing Authorities, Australia;

N/E Not encountered;

Nested structures* A *regionalised variable* whose spatial continuity is the compound effect of several genetic sources of spatial variation;

Noise spikes A phenomenon associated with measurements of q_c and f_s that occurs randomly, and as a result of electrical noise originating from inadequate earthing of the *CPT* cable (cf. Figure 3.15);

Nugget effect When the *semivariogram* does not pass through the origin and arises from the *regionalised variable* being so erratic over a short distance that the *semivariogram* goes from zero to the level of the nugget in a distance less than the sampling interval;

OLS The regression analysis method of ordinary least squares;

Ordinary kriging The general geostatistical estimation process often simply known as *kriging*. Unlike *simple kriging*, the mean is unknown;

Overshoot The amount of output measured beyond the final steady output value in response to a step change in the *measurand*;

PACF Partial autocorrelation function;

PC Personal computer;

Permanent mark A rigid reference point whose *AMG* and *AHD* coordinates are known accurately;

PLT Plate load test;

RAM Random access memory;

Random field* A collection of random variables in an *n*-dimensional euclidean space;

Random field theory The application of *time series analysis* to the spatial variability of geotechnical properties, and unlike *time series analysis*, random field theory is not confined to one dimension;

Range of influence* The maximum distance separating pairs of random variables that have any significant statistical dependence;

Rationalised depth A depth below the ground surface which refers to the *CPT*, and which has been rounded to the nearest 5 mm;

RAW An irrigation/soil science parameter which measures the water reservoir of the soil between full point, –8 kPa, and refill point, –60 kPa, and is expressed in mm (Brooker et al., 1995);

Rebound phenomenon A phenomenon observed in measurements of f_s within the Keswick Clay at the depth at which the test is temporarily suspended and later recommenced. It is manifested by a sudden increase in measurements of f_s below the depth at which the test was suspended. It is proposed that this phenomenon is a consequence of rebound of the pseudo-overconsolidated Keswick Clay, and which would not have occurred had the test not been suspended;

Regionalised variable A variable which has properties that are partly random and partly spatial, and has continuity from point to point, but the changes are so complex that it cannot be described by a tractable deterministic function;

Relative nugget The ratio between the *nugget effect*, C_0, and the level of the sill, $C + C_0$;

Resolution The magnitude of discernable (detectable) output changes as the *measurand* is continuously varied over the range;

RL Reduced level;

RMA The regression analysis method of reduced major axis;

SBPT Self-boring pressuremeter test;

Scatterplot An *x*-*y* graph on which the *x*-coordinate corresponds to the value of one variable and the *y*-coordinate corresponds to the value of the other variable;

SDF *Spectral density function*;

Semivariogram, g The expected value, or mean, of the squared difference between pairs of points, Y_x and Y_{x+h}, separated by a displacement, *h*;

Shift distance The distance by which f_s measurements are shifted, usually 75 mm, so that measurements of q_c and f_s correspond to the same depth. Such a shift enables the calculation of F_R to be performed correctly;

Sill* The limiting value of the *semivariogram* which is reached at some finite distance known as the *range of influence*. The sill is numerically equal to the variance of the random function;

Simple kriging* The same as *ordinary kriging*, except that the mean is known, and hence the final row is deleted from all matrices, as is the final column of the square matrix;

Skew., skewness The skewness is a measure of the symmetry of a data distribution. A skewness of zero suggests a symmetrical distribution, a positive value indicates a right-hand skew, and a negative value indicates a left-hand skew;

Spatial series A sequence of discrete or continuous data measured at specific locations - the spatial equivalent of a *time series*;

Spectral density function The Fourier transform of the *ACF*; that is, in the frequency domain;

SPLT Screw plate load test;

Stationarity* A term used to denote different degrees of invariance in the characteristics of *random fields*. If the mean and autocovariance of the series change with the lag, and not location, the series is said to be ***weakly stationary***. If all higher moments depend on the lag, and not position, the series is said to be ***stationary in the strict sense***. (cf. *homogeneity*);

Stiction The resistance to movement developed between the writing mechanism and the paper of a chart recorder, resulting in a delayed response to input signals;

TCD# Consolidated drained triaxial test with # stages;

TCU# Consolidated undrained triaxial test with # stages;

Time series* A sequence of discrete or continuous data measured at specific instances in time - also a 1D *random field* (cf. *spatial series*);

Time series analysis A mathematical technique used to estimate properties which are temporally or spatially dependent. When applied to geotechnical engineering, time series analysis is usually referred to as *random field theory*;

Transitive semivariogram* A *semivariogram* with a finite *sill*. For example, the spherical, exponential and Gaussian models are all types of transitive semivariograms;

Trend* An abstract expression of the low frequency, large-scale systematic variation of a *regionalised variable*. The trend may also include bias in the test method (cf. *drift*);

TUC Unconfined triaxial test, or, unconfined compression test;

TUU# Unconsolidated undrained triaxial test with # stages;

UC Universal column - a mild steel I beam primarily used as a compression member;

UCS Unconfined compressive strength;

Universal kriging* *Simple kriging* of the residuals of a *regionalised variable* after automatically removing optimal estimates of the *drift*, and is used for non-*stationary* data, that is, when a deterministic *trend* exists in the measured data;

USCS Unified soil classification system;

UU Unconsolidated undrained triaxial test;

VST Vane shear test.

CORRIGENDA

"The Influence of Spatial Variability on the Geotechnical Design Properties of a Stiff, Overconsolidated Clay"

by M. B. Jaksa

March 1996

---

pg. *vii*, **Acknowledgments** *After 3rd paragraph add:*

"In addition, I am grateful for the generosity and assistance provided by Australian National, and in particular, Mr. Peter Gaskill, for allowing testing to be carried out at the Keswick site. I also wish to thank Dr. K. S. Li, Mitchell, McFarlane, Brentnall and Partners, Hong Kong, and Dr. S.-C. R. Lo and Mr. G. R. Mostyn, University of N.S.W., for permission to use the program *PROBSN*."

pg. 231, Table 5.12: *Replace* "kN/m^3" *with* "kN/m^2"

pg. 269, Para. 2, Line 2: *Replace* "from 6% to 41%" *with* "from 5% to 22%"

pg. 270, Table 5.22 *Replace Random Field Theory table with* (values which have been corrected are shown in **bold**):

Random Field Theory

Degree of Polynomial Trend Removed from Data	**Kendall's τ Test**	**Degree of Fit, r^2**	**r_B (mm)**	**r_1**	**r_0**	**ACF Nugget, R_0**
None	×	-	**765**	**0.95**	**0.95**	**5%**
1	×	0.088	680	0.94	0.94	6%
2	✓	0.719	240	**0.88**	**0.88**	**12%**
3	✓	0.730	190	0.88	0.88	12%
4	✓	0.774	190	0.87	0.87	13%
5	✓	0.818	110	0.86	0.86	14%
6	✓	0.846	85	0.78	0.78	22%

pg. 271, Figure 5.86 *Replace Figure 5.86(a) with*:

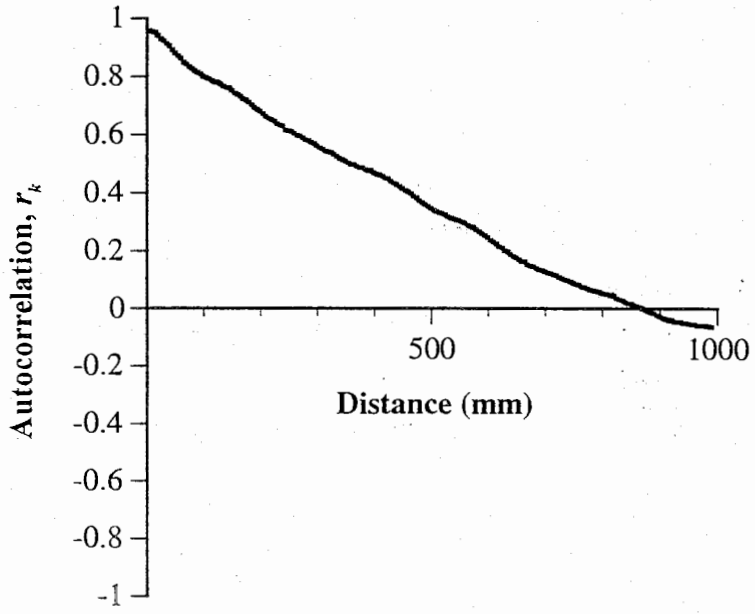

pg. 274, Para. 4, Line 2: *Replace:* "substantially, from 3% to 56%, and again demonstrates that the nugget depends greatly on the degree of trend which is removed from the data"
With: "varies only marginally, from 3% to 4%."

pg. 275, Table 5.24 *Replace Random Field Theory table with* (values which have been corrected are shown in **bold**):

Random Field Theory

Degree of Polynomial Trend Removed from Data	Kendall's τ Test	Degree of Fit, r^2	r_B (mm)	r_1	r_0	ACF Nugget, R_0
None	×	-	**1,075**	**0.97**	**0.97**	**3%**
1	✓	0.047	655	0.97	0.97	3%
2	✓	0.184	135	0.97	0.97	3%
3	✓	0.297	110	0.97	0.97	3%
4	✓	0.379	100	0.96	0.96	4%
5	✓	0.384	100	0.96	0.96	4%
6	✓	0.394	95	0.96	0.96	4%

pg. 278, Para. 3, Line 4: *Replace* "56%" *with* "22%"

pg. 356, Line 4: *Replace the last occurrence of* "F5A" *with* "F51"